HHS Public Access

Author manuscript

Oncogene. Author manuscript; available in PMC 2016 October 28.

Published in final edited form as:

Oncogene. 2016 October 27; 35(43): 5597–5607. doi:10.1038/onc.2016.101.

Osteocytic Connexin Hemichannels Suppress Breast Cancer Growth and Bone Metastasis

Jade Z. Zhou[1], **Manuel A. Riquelme**[1], **Sumin Gu**[1], **Rekha Kar**[1], **Xiaoli Gao**[1], **LuZhe Sun**[2,3], and **Jean X. Jiang**[1,3,*]

[1]Department of Biochemistry, University of Texas Health Science Center, 7703 Floyd Curl Drive, San Antonio, Texas 78229-3900, USA

[2]Department of Cellular and Structural Biology, University of Texas Health Science Center, 7703 Floyd Curl Drive, San Antonio, Texas 78229-3900, USA

[3]Cancer Therapy and Research Center, University of Texas Health Science Center, 7703 Floyd Curl Drive, San Antonio, Texas 78229-3900, USA

Abstract

Although the skeleton is one of predominant sites for breast cancer metastasis, why breast cancer cells often become dormant after homing to bone is not well understood. Here, we reported an intrinsic self-defense mechanism of bone cells against breast cancer cells: a critical role of connexin (Cx) 43 hemichannels in osteocytes in the suppression of breast cancer bone metastasis. Cx43 hemichannels allow passage of small molecules between the intracellular and extracellular environments. The treatment of bisphosphonate drugs, either alendronate (ALN) or zoledronic acid (ZOL), opened Cx43 hemichannels in osteocytes. Conditioned media (CM) collected from MLO-Y4 osteocyte cells treated with bisphosphonates inhibited the anchorage-independent growth, migration and invasion of MDA-MB-231 human breast cancer cells and Py8119 mouse mammary carcinoma cells and this inhibitory effect was attenuated with Cx43(E2), a specific hemichannel blocking antibody. The opening of osteocytic Cx43 hemichannels by mechanical stimulation had similar inhibitory effects on breast cancer cells and this inhibition was attenuated by Cx43(E2) antibody as well. These inhibitory effects on cancer cells were mediated by ATP released from osteocyte Cx43 hemichannels. Furthermore, both Cx43 osteocyte-specific knockout mice and osteocyte-specific Δ130–136 transgenic mice with impaired Cx43 gap junctions and hemichannels showed significantly increased tumor growth and attenuated the inhibitory effect of ZOL. However, R76W transgenic mice with functional hemichannels but not gap junctions in osteocytes did not display a significant difference. Together, our studies establish the specific inhibitory role of osteocytic Cx43 hemichannels, and exploiting the activity of this channel could serve as a de novo therapeutic strategy.

*Corresponding author: Jean X. Jiang, Ph.D., Department of Biochemistry, University of Texas Health Science Center, 7703 Floyd Curl Drive, San Antonio, TX 78229-3900, Tel: 210-562-4094; Fax: 210-562-4129, jiangj@uthscsa.edu.

Conflict of Interest

The authors declare no conflict of interest.

Keywords

connexin hemichannels; osteocytes; breast cancer; bone metastasis

INTRODUCTION

Cancer progression frequently leads to bone metastases, which are serious complications occurring in approximately 70% of patients with advanced breast cancers. Bone metastases cause significant complications, and quality of life is greatly compromised [1,2]. Many features, including increased blood flow as well as the release of growth factors, cell adhesion molecules, and chemoattractants from cells in the bone matrix, account for the frequency of bone metastases [3,4]. In recent years, the cancer cell microenvironment has been recognized as a crucial contributor to tumor progression [5]. Bone tissue is made up of three major cell types: osteocytes, osteoblasts, and osteoclasts. Osteocytes, comprising over 95% of total bone cells, are the most abundant cell type in the bone and are important in mediating bone mechanical sensitivity and maintaining homeostasis by coordinating the activities of osteoclasts and osteoblasts [6,7]. In breast cancer skeletal metastases, there is a close correlation between bone destruction and tumor growth [4]. A majority of prior studies point to the contribution of the bone microenvironment in favor of tumor growth and metastasis; however, the intrinsic, potential anti-neoplastic properties of bone cells are largely unexplored.

Osteocytes amply express connexin (Cx) proteins, which form both gap junction channels and hemichannels. Gap junction channels mediate the intercellular communication between two adjacent cells, whereas hemichannels permit the exchange of molecules between cells and the extracellular environments [8,9]. These Cx-forming channels permit small molecules (<1.2 kDa) such as NAD^+, glutamate, ATP and inositol triphosphate (IP3) to pass through [10,11]. Cx43 is the most predominantly expressed connexin found in osteocytes. We and others have shown that osteocytic Cx43 hemichannels are responsive to mechanical loading and alendronate (ALN) [12,13,14,15], a bisphosphonate drug commonly used to treat bone diseases and metastases [16], to release ATP and prostaglandins[12,13,14,15.]

Cx43 as well as several other connexins have long been known to inhibit tumor cell growth and progression; however these previous studies primarily focus on the expression and roles of connexin within the cancer cells [17,18,19]. Clinical studies show that deficient or abnormal connexins are frequently found in tumor tissues and cell lines, such as breast cancer, prostate cancer, lung cancer, and many other cancers [18]. For example, Cx43 was found to be reduced in breast carcinoma cells obtained from the primary tumors of breast cancer patients [20]. Furthermore, the attachment of breast cancer cells to the pulmonary endothelium is increased with the overexpression of Cx43 in breast cancer cells, which enhances the adhesion of the cancer cells to the lung endothelial cells [21]. Breast cancer cells also use Cx43 to initiate brain metastatic lesions by forming gap junctions with the endothelial cells in the vasculature, whereas inhibition of the connexins by RNAi or pharmacological methods inhibited brain colonization [22]. Several *in vivo* studies indicate the possible tumor suppressive roles of Cx43 in the cancer microenvironment; mice with reduced Cx43

expression display increased tumor growth and metastasis in the lung [23,24]. However, there are no preceding studies establishing the functional involvement of Cx43 channels in host cells and how they influence cancer cell proliferation, migration, and metastasis. This study demonstrates that the opening of Cx43 hemichannels in osteocytes, either by bisphosphonate treatment or by mechanical stimulation, inhibits the migration, invasion and growth of breast cancer cells. Furthermore, we utilize several Cx43 mouse models: a Cx43 osteocyte-specific knockout mouse model and two Cx43 osteocyte-specific transgenic mouse models, R76W and Δ130–136, which contain functional hemichannels but impaired gap junctions, or both nonfunctional hemichannels and gap junctions, respectively. These *in vivo* models reveal the specific inhibitory influence of Cx43 hemichannels against breast tumor progression and suggest that osteocytic Cx43 hemichannels exert a significant self-protective mechanism of bone tissue against the colonization and expansion of breast cancer cells through osteocytic Cx43 hemichannels.

RESULTS

The opening of osteocytic Cx43 hemichannels by bisphosphonates inhibits the migration, invasion and anchorage-independent growth of breast cancer cells

To determine if osteocytes are involved in mediating the effect of ALN on suppression of breast cancer cells, we treated osteocytic MLO-Y4 cells with ALN and collected the CM. Using the wound healing migration assay, we found that the CM from MLO-Y4 osteocytes treated with ALN (CM-ALN) significantly decreased the migration of MDA-MB-231 breast cancer cells in a dose-dependent manner (Fig. 1A). To eliminate the possibility that this effect is due to changes in cell proliferation, the WST-1 cell proliferation assay was performed under the identical treatment as the cell migration assay. There was no significant difference in the proliferation of the MDA-MB-231 cells with CM from MLO-Y4 cells treated with 0–20 μM ALN whereas at 60 μM ALN CM, the cells exhibited increased proliferation (Fig. S1). Accordingly, we used CM from MLO-Y4 cells treated with 20 μM ALN in later experiments. We also observed a significant decrease in MDA-MB-231 cell invasion with the CM collected from MLO-Y4 cells with 20 μM ALN (Fig. 1B). As further assurance that the decrease in migration is not a direct effect of ALN on the MDA-MB-231 cell migration, we added ALN directly to the cancer cells. In this case, the cells did not exhibit a significant difference in migration with varying concentrations of ALN (Fig. 1C), demonstrating that ALN does not directly affect the cell migration. Together, these results showed that the CM collected from ALN-treated osteocytes cause a significant inhibition of MDA-MB-231 breast cancer cell migration and invasion.

To test if the opening of Cx43 hemichannels in osteocytes induced by ALN (Fig. S2A) [25] mediates the inhibitory effect of CM collected from MLO-Y4 cells on the MDA-MB-231 cells, we used a hemichannel-blocking antibody, Cx43(E2), which targets the second extracellular loop (E2) of Cx43 [14,26]. We observed a complete attenuation of the decrease in wound healing migration of MDA-MB-231 cells with the CM from MLO-Y4 cells treated with both Cx43(E2) antibody and ALN (Fig. 2A). A similar observation was obtained when using the transwell migration assay with the MDA-MB-231 cells (Fig. 2B). A similar inhibitory effect of the CM was observed on migration of Py8119 (Fig. 2C), a mouse

mammary carcinoma cell line which can grow and metastasize in immunocompetent mice [27]. Cell proliferation was not affected by these treatments (Fig. S3).

To define the specificity of osteocytes and also Cx43 hemichannels, we tested the MLO-A5 osteoblastic cell line, which was generated using a similar strategy as the MLO-Y4 cells [28]. Cx43 is abundantly expressed in MLO-A5 cells (Fig. S2C) [29]. However, unlike MLO-Y4 cells, ALN did not induce the opening of hemichannels (Fig. S2B). Consistently, we did not observe differences in migration of MDA-MB-231 cells when they were incubated in CM collected from MLO-A5 cells treated with or without ALN and/or Cx43(E2) antibody (Fig. 2D). There was also no difference in cell proliferation (Fig. S4).

To determine the effect of CM-ALN on the anchorage-independent growth of breast cancer cells, we cultured the MDA-MB-231 cells in soft agar. Similar to their effects on cell migration, the CM from MLO-Y4 osteocytes treated with ALN significantly decreased the colony formation of MDA-MB-231 cells in a dose-dependent manner (Fig. 3A, bottom panel). Furthermore, the CM from 20 μM ALN-treated MLO-Y4 cells significantly inhibited the MDA-MB-231 cells colony formation on soft agar, while the addition of Cx43(E2) antibody significantly reversed the effect (Fig. 3B). To ensure objectivity in quantifying the extent of tumor growth and to account for variation in colony sizes (the diameter of each colony) in the soft agar colony formation assay, we measured the colony sizes and demonstrated that while CM-ALN treatment reduced the number of colonies in soft agar, it did not change colony size distribution (Fig. S5). These results show that CM-ALN truly decreased MDA-MB-231 cell colony formation and suggest that the explicit opening of Cx43 hemichannels on MLO-Y4 cells with the release of inhibitory factors decreased breast cancer cell migration and anchorage-independent growth.

To examine whether other bisphosphonate drugs have a similar effect as ALN on osteocytic Cx43 hemichannels, we tested zoledronic acid (ZOL), one of the most potent and commonly prescribed bisphosphonate drugs in the treatment of bone metastasis [30,31]. A significant dose-dependent increase in dye uptake of MLO-Y4 cells with ZOL is observed (Fig. 4A). Similar to ALN, the CM from MLO-Y4 cells treated with ZOL decreased MDA-MB-231 cell migration, whereas the addition of Cx43(E2) antibody caused a significant attenuation of the effect (Fig. 4B). There was no significant difference in cell viability as observed with the WST-1 assay (Fig. 4C). Therefore, Cx43 hemichannels on MLO-Y4 cells are similarly stimulated by ZOL, leading to the release of inhibitory factors in the suppression of breast cancer cell migration.

We recently found that ATP released by osteocytes is responsible for the inhibitory effect of bisphosphonates on breast cancer cell growth, migration and metastasis [32]. The levels of ATP in the CM were measured by liquid chromatography–mass spectrometry (LC-MS). The treatment with 20 μM ZOL for 24 hrs significantly increased the ATP release and this release is completely inhibited by Cx43(E2) antibody (Fig. 4D). This data suggest that the inhibitory effect of osteocytic Cx43 hemichannels on breast cancer cells is mediated primarily via ATP released from these channels.

The opening of osteocytic Cx43 hemichannels by mechanical stimulation inhibits the migration of breast cancer cells

Osteocytes are the principal mechanosensor cells of bone [33,34]. Fluid flow shear stress, a major form of mechanical stimulation sensed by osteocytes, activates osteocytic Cx43 hemichannels, allowing the release of bone anabolic factors [12,35]. Using the parallel plate flow chamber [36], MLO-Y4 cells were subjected to shear stress levels and subsequently, the fluid flow CM (CM-FF) was collected. CM-FF from MLO-Y4 cells exposed to fluid flow at 16 dyn/cm^2 for 2 hr or 16 hr significantly decreased the migration of MDA-MB-231 cells by over 60% or nearly 90%, respectively (Fig. 5A). When MLO-Y4 cells were incubated with Cx43(E2) antibody and subjected to FFSS, the produced CM was ineffective in decreasing MDA-MB-231 migration. The cell viability of MDA-MB-231 cells during the time period used in the transwell assay did not decrease when treated with CM-FF; instead, an increase was observed (Fig. 5B). Consistently, there was a significant decrease in MDA-MB-231 cell invasion with the treatment of CM-FF (Fig. 5C). These results suggest that the opening of Cx43 hemichannels in osteocytes exerts major inhibitory effects on breast cancer cells regardless of the method either by pharmacological reagents or mechanical stimulation.

Increased tumor growth and metastasis of mouse mammary carcinoma cells in osteocyte-specific Cx43 knockout and Cx43 hemichannel-deficient transgenic mouse models

Given that our *in vitro* data suggest that osteocytic Cx43 hemichannels play an important role in the suppression of anchorage-independent growth, migration and invasion of breast cancer cell, we used a Cx43 osteocyte-specific conditional knockout mouse model to corroborate the results *in vivo*. Cx43 expression was greatly reduced in the bone tissues of Cx43 conditional knockout mice (Cx43 cKO) (DMP1-Cre; Cx43$^{fl/-}$) (Fig. S6A). Consistent with a previous report of Cx43 cKO controlled by an 8-kb DMP-1 promoter [37], there is no alteration of bone mineral density (BMD) between WT and Cx43 cKO (Fig. S6B). Py8119 mouse mammary carcinoma cells were injected into the right tibias of both WT control and Cx43 cKO mice. The tumor growths were monitored with whole animal imaging once a week for 4 weeks. Bioluminescence analysis revealed that the Cx43 cKO mice had significantly increased tumor growth compared to the WT mice, particularly in week 4, as reflected by bioluminescence signals from both the ventral (Fig. 6A) and dorsal (Fig. 6B) positions. Quantification of the bioluminescence signals further confirmed the increase of tumor growth (Fig. 6, A and B, lower panels). Furthermore, tumor cells were found to spread to the lungs and brain of the Cx43 cKO mice (Fig. 6A, middle panels). X-ray radiography shows that osteolytic lesion formation in the bone as a result of tumor growth is more evident in the Cx43 cKO than WT mice (Fig. 6C). These results suggest a protective role of Cx43 in osteocytes against breast cancer cells *in vivo*.

To further define the roles of Cx43 hemichannels *in vivo*, we recently developed two transgenic mice expressing dominant negative Cx43 in osteocytes [38]. We have shown that the Cx43(R76W) mutant dominant-negatively blocks the formation of functional gap junctions only and not hemichannels, whereas the Cx43(Δ130–136) mutant blocks both functional gap junctions and hemichannels formed by endogenous Cx43 in osteocytes. Py8119 cells were injected into the right tibia of WT, Cx43(R76W) and Cx43(Δ130–136) transgenic mice. Bioluminescence analysis of the animals demonstrated no difference in

tumor growth when comparing Cx43(R76W) with WT mice (Fig. 7A). However, Cx43(Δ130–136) mice displayed increased tumor growth compared to WT and Cx43(R76W) mice. Quantification of the bioluminescence signals further confirmed the differences of tumor growth in bone of the Cx43(Δ130–136) mice. To test if the inhibitory effect of bisphosphonates on bone metastasis is primarily mediated by Cx43 hemichannels in vivo, WT and Cx43(Δ130–136) mice were intratibially implanted with Py8119 cells and then treated with ZOL. Tumor growth was significantly decreased in WT mice treated with ZOL; however, this decrease was basically lost in Cx43(Δ130–136) (Fig. 7B). This data further suggests a specific role of Cx43 hemichannels in the protection of osteocytes against breast cancer growth and metastasis in the bone and in mediating the tumor suppressive function of bisphosphonates.

DISCUSSION

Cancer metastasis is a complex and adaptive process which is highly influenced by the cell environment [39]. Bone is one of the most preferred sites for cancer metastasis [2]. Many studies demonstrate that the tissue tropism of bone by metastatic tumor cells from breast, prostate and lung cancers is influenced by interactions between the circulating tumor cells and the cells of the bone tissue [40]. It has long been thought that the microenvironment of the local tissue actively contributes to the propensity of certain cancers to metastasize to secondary organs, and that bone provides a particularly fertile “soil” [41]. Bone cells mediate the release of various cytokines and growth factors which influence the behavior of cancer cells [2]. Osteocytes embedded in bone mineral matrix make up a majority of total bone cells and have important roles as the mechanosensors and bone remodeling coordinators of the bone [42]. However, their role in bone metastasis remains essentially unknown. Cx43 hemichannels, which are abundantly expressed in osteocytes, have low activity under normal, non-stimulating conditions. In response to stimuli such as bisphosphonates and mechanical loading, Cx43 hemichannels found in osteocytes are known portals for the release of molecules such as PGE_2 and ATP [15,12,13,14]. It is well known that connexin hemichannels open in response to different physiological conditions and pathological stimuli to elicit numerous processes, including paracrine signaling, cell death, inflammation, and neuronal communication [10,43]. The release of ATP by Cx43 hemichannels is implicated in the signaling and metabolic control of early inflammatory response by endothelial cells, as well as by polymorphonuclear leukocytes during activation [21,44]. We have recently reported that ATP released by osteocytes exerts an inhibitory effect on breast cancer bone metastasis [32]. This study, for the first time shows that osteocytic Cx43 hemichannels play a critical role in influencing cancer progression and metastasis.

Cx43 is required for bone development, modeling and remodeling, and mutations can cause bone disorders such as oculodentodigital dysplasia (ODDD), an autosomal dominant human disease, characterized by craniofacial bone abnormalities and limb deformities [45,46]. To study the precise role of Cx43 in specific bone cells, several conditional knockout mice have been generated using Cre recombinases which are driven by specific promoters found in osteoprogenitors, osteoblasts, or osteocytes. For example, mice with an osteoblast specific deletion of Cx43 using the collagen type I Cre recombinase demonstrated low bone mass and decreased bone formation, as well as osteoblast dysfunction and attenuated response to

PTH (parathyroid hormone), an important hormone in calcium homeostasis and bone remodeling [47]. Osteocyte-specific Cx43 knockouts driven by a DMP1 promoter displayed increased osteocyte apoptosis, endocortical resorption and periosteal bone formation, resulting in reduction in mineralization and higher bone marrow cavity, as well as increased osteogenic response to mechanical stimulation, which was found to be associated with increased levels of β-catenin [37, 48]. In studies of mice with a Cx43 deletion in both osteoblasts and osteocytes, the mutant mice exhibited increased bone loss due to augmented bone resorption and osteoclastogenesis [49,50]. These mice also demonstrated delayed bone formation and healing during fracture healing [50]. Furthermore, the Cx43 deficient mice displayed enhanced anabolic response to mechanical loading [49]. The aforementioned studies all clearly demonstrate the critical role that Cx43 plays in the bone microenvironment.

In this study, we demonstrate that osteocytic Cx43 hemichannels play a key role in the inhibition of breast cancer cell migration, invasion and tumor growth in the bone microenvironment. Here, we used both the wound healing and transwell migration assays to examine breast cancer cell migration. The decrease in migration of cancer cells by the CM collected from bisphosphonate- or FFSS-treated osteocytes were not due to alterations of cell proliferation and viability. In addition to its inhibitory effect on cancer cell migration, osteocytic Cx43 hemichannel opening inhibits the anchorage-independent growth of breast cancer cells in soft-agar matrix. Thus, the opening of Cx43 hemichannels in osteocytes reduces breast cancer cell progression through the inhibition of migration, invasion, and growth.

Cx43 is able to form both gap junctions and hemichannels, and most of the known chemical inhibitors block both types of channels. We have developed an antibody, Cx43(E2) that targets the second extracellular loop domain of Cx43. Our lab previously demonstrated through scrape-loading dye transfer and dye uptake induced by FFSS, that Cx43(E2) antibody is specific to hemichannels, but has minimal effects on gap junctions [14]. This is the only antibody available for specifically blocking Cx43 hemichannels [14,26]. By using this antibody, other laboratories have shown the specific inhibition of Cx43 hemichannels in brain cells [51,52,53]. Here, we used Cx43(E2) antibody to demonstrate that the inhibitory effect on breast cancer cell growth and migration is primarily mediated by osteocytic Cx43 hemichannels. The specific effect of Cx43 hemichannels in osteocytes is also proven by using MLO-A5 osteoblastic cells. This cell line was established using a similar approach as MLO-Y4 osteocyte cells [54,28]. MLO-A5 cells express similar levels of Cx43 on the cell surface and inside the cell as MLO-Y4 cells [29], but we failed to detect functional hemichannels. We showed here that ALN failed to induce the opening of Cx43 hemichannels in MLO-A5 cells. Thus, it is not surprising that CM collected from this osteoblastic cell with ALN treatment cannot suppress human breast cancer cell progression. We sought additional validation of the effect of Cx43 hemichannels on breast cancer cells by using a murine mammary carcinoma cell line. A similar inhibitory effect of CM from ALN-treated osteocytes was obtained which was not due to changes in cell viability. Therefore, osteocyte Cx43 hemichannels specifically influence the behavior of both human and mouse mammary carcinoma cells.

We recently reported that ATP released by osteocytes is a mechanism underlying the inhibitory role of bisphosphonates in breast cancer cells [32]. Several studies have established the anti-neoplastic function of extracellular ATP to inhibit several cancer cell lines, including prostate cancer cells, colon adenocarcinoma cells, melanoma cells, and bladder cancer cells [55,56,57]. Cx43 hemichannels are permeable to ATP in osteocytes, astrocytes and other types of cells [13,58,59,60]. Consistently, we showed that the release of ATP by bisphosphonates was completely diminished by the specific inhibition of Cx43 hemichannels via Cx43(E2) antibody. Moreover, this antibody also totally abolishes ATP release in the absence of bisphosphonates, suggesting that Cx43 hemichannels in osteocytes are primarily responsible for ATP release. The treatment of bisphosphonates towards increasing the activity of hemichannels greatly elevates extracellular ATP level. As we have shown earlier, ATP acts via the activation of purinergic receptors and suppresses breast cancer growth, migration and metastasis *in vitro* and *in vivo*[32].

The intravenous bisphosphonates, pamidronate and ZOL, are FDA approved for the treatment of bone metastases. Although not FDA approved, other bisphosphonates such as clodronate and ibandronate are used in other countries and have shown to be effective. Our results showed that ZOL stimulated the opening of Cx43 hemichannels in MLO-Y4 cells, and the CM collected from ZOL-treated MLO-Y4 cells inhibited the migration of MDA-MB-231 breast cancer cells to an even greater degree than the CM-ALN, while Cx43(E2) antibody attenuated the effect. Recent studies have demonstrated various side effects that patients who take bisphosphonates may incur, including renal toxic effects and osteonecrosis of the jaw [16,61]. These discoveries have necessitated an exploration for alternatives to treat bone metastasis.

Physical exercise has shown promise as adjuvant therapy for breast cancer patients [62,63]. Many studies have reported encouraging outcomes of exercise and physical activity on reduction of tumor growth and metastasis [62,64]. In particular, several epidemiology studies have found a substantial beneficial association between regular physical activity and survival, in that women who engaged in exercise activity after breast cancer diagnosis had a significantly reduced risk of dying from breast cancer [64]. Results from the Women's Health Initiative also reported significantly decreased cancer-related mortality in postmenopausal women diagnosed with invasive breast cancer who participated in physical activity [65]. Moreover, a recent *in vivo* mouse study showed that mechanical loading via tibial compression for 6 weeks after intratibial injections of MDA-MB-231 cells dramatically reduced osteolysis and tumor formation [66]. Osteocytes are major mechanosensory cells in the bone, and fluid flow is a major type of mechanical stimulation on osteocytes [34]. Cx43 hemichannels in osteocytes are highly sensitive to mechanical loading [12,13]. We showed here that opening of osteocytic Cx43 hemichannels, regardless of the stimuli either by bisphosphonates or mechanical loading, is critical for the inhibitory effect on breast cancer cells.

We used several *in vivo* murine models to evaluate the inhibitory roles of Cx43 and hemichannels in osteocytes in breast cancer. The first model is Cx43 cKO mice driven by a 10-kb DMP1 promoter. A Cx43 osteocyte-specific cKO model driven by the 8-kb DMP1-Cre has been reported by another group [37]. Similar to our observation, they found increased

empty lacunae in the cortical bones associated with more osteocytes under apoptosis. We used intratibial injections, a common method used to study bone metastasis after tumor cells have entered the bone, mimicking the late stage of bone metastasis [67]. Intratibial Py8119 tumor growth was augmented in this knockout model. Moreover, in some mice, the tumor cells spread to brain and lung tissues. Like the Cx43 DMP1-Cre;Cx43fl/fl mice, we also observed the incidence of metastatic lesions outside the bone of the Δ130–136 mice (data not shown). One possibility is that endogenous Cx43 protein level may be altered in these transgenic mouse models. However, we did not observe the alteration of endogenous Cx43 level in the brain in Δ130–136 mice as compared to WT control (Fig. S7). We could not detect Cx43 protein in the lung due to its low abundance in that tissue. Metastasis to other organs in this knockout model further indicates that a possible “barrier” function of the bone tissue is compromised given the fact that the tumor cells were implanted originally in the bone marrow cavity. This possibility is further supported by the increased osteolytic lesions in the tibias of the Cx43 cKO mice.

The limitation of using knockout mice is that such approaches deplete both gap junction channels and hemichannels formed by Cx43, which makes it difficult to distinguish the action of these two types of the channels. Therefore, we used two transgenic mouse models: R76W mice, which harbor dominant-negatively impaired Cx43 gap junctions, while Δ130–136 mice have both types of channels impaired [68]. The mice with both impaired gap junctions and hemichannels (Δ130–136) have greatly enhanced osteolytic tumor growth, whereas the mice with functional hemichannels (R76W), despite impaired gap junctions, do not have a significant difference in tumor growth compared to the wild-type mice. In the transgenic models, Cx43 remains present on the cell surface, and its potential role in intercellular adhesion cannot be excluded. However, we did not observe such effects in the R76W mice which form only functional hemichannels and not gap junctions, although this mutant is also expressed on the cell surface. This indicates that intercellular adhesion does not play a predominant role in facilitating metastasis. More importantly, the tumor suppressive response of WT mice to ZOL treatment as evidenced by the reduction of tumor growth is very much attenuated in Δ130–136 mice. These mouse models not only help demonstrate the importance of Cx43 expression in osteocytes through the Cx43 osteocyte-specific conditional knockout mice (Cx43 cKO), but also Cx43 hemichannel function, through the transgenic mice.

Connexins are known to be essential in cell proliferation, differentiation, and tissue homeostasis [69]. However, the role of connexins in cancer development and advancement is contentious and not readily reconciled. Bone osteocytes richly express Cx43 hemichannels, and these channels are sensitive to mechanical stimulation and bisphosphonates. As discussed above, both treatments are known to be involved in the suppression of bone metastasis. Overall, our *in vitro* and *in vivo* study demonstrated that Cx43 hemichannels have an intrinsic protective role against breast cancer cell anchorage-independent growth, migration and metastasis process. The results from these studies have significant clinical implications in providing a foundation to explore improved treatments for breast cancer bone metastases. The global increase of Cx43 hemichannel uptake may not be a practical therapeutic strategy due to the detrimental effects in other tissues. However, the specific activation of these hemichannels in osteocytes may be a feasible target for cancer

therapeutics. Most breast cancer related deaths are associated with metastasis, and understanding how Cx43 hemichannels in osteocytes and ATP specifically contribute to this process may pave the way for new advances in breast cancer therapeutic intervention.

MATERIALS AND METHODS

Cell cultures and conditioned media (CM) preparation

MDA-MB-231 cells were cultured in McCoy's 5A modified media with 10% fetal bovine serum (FBS). Murine mammary carcinoma Py8119 cells were grown in F12K nutrient media with 5% fetal clone II. Murine osteocytic MLO-Y4 cells seeded on rat tail collagen type I (BD Biosciences, San Jose, CA) coated plates were grown in α-modified essential medium (α-MEM) with 2.5% FBS and 2.5% bovine calf serum (BCS). All cell lines were cultured under 5% CO_2 and 37°C.

MLO-Y4 cells were cultured for 24 hr, after which media was changed with α-MEM without phenol red with 2.5% FBS and 2.5% BCS. MLO-Y4 cells were incubated in the absence or presence of alendronate (ALN) (4-amino-1-hydroxybutylidene-1, 1-bisphosphonic acid) or zoledronic acid (ZOL) (1-Hydroxy-2-(1H–imidazol-1-yl)ethylidene, bisphosphonic acid) and/or Cx43(E2) antibody, a rabbit polyclonal antibody developed in the lab [14] for 48 hr, and the CM was collected.

Dye uptake

The cells were treated with or without ALN or ZOL for 30 min in absence or presence of 1 μg/ml Cx43(E2) antibody and then with recording medium (α-MEM+10 mM HEPES) containing ethidium bromide (EtBr) 50 μM for 5 min and fixed with 2% paraformaldehyde (PFA). At least three microphotographs of fluorescence fields were taken with an inverted microscope (Carl Zeiss) with a rhodamine filter and analyzed by ImageJ software. Defined circular regions of interest (ROI) (over nucleus) were used to measure the average pixel density of 30 random cells.

Wound healing assay

MDA-MB-231 cells were seeded onto sterile 6-well plates and allowed to form a confluent cell monolayer per well (> 95% confluence). Wounds were created in each cell monolayer using a sterile 10 μl pipette tip. After the initial images were taken, the cells were incubated for 24 hr at 37°C, after which images of the wound areas were taken again. Cell migration was quantitatively measured by the gap area using WCIF ImageJ software; the values obtained were expressed as % of covered wound.

Transwell migration and invasion assays

Transwell migration was performed as previously described [70]. Invasion assays were performed with the BD Biocoat growth factor reduced Matrigel invasion chambers kit in 24-well tissue culture plates. Five-hundred microliter breast cancer cell suspensions were added to the upper side of the chambers at a density of 1×10^5 cells/insert and 750 μl CM was added to the lower wells. The number of migrated cells in 5 fields of view per insert was

counted under a light microscope at magnification 10 X. Experiments were carried out in triplicate.

WST-1 cell viability and soft agar colony formation

Cancer cell proliferation was assessed using WST-1 (Water Soluble Tetrazolium salts) assay kit (Roche, Basel, Switzerland) as previously described [32]. Briefly, a cell suspension was plated in 96-well plates at 2×10^4 cells/well. The cell proliferation was measured at an emission wavelength of 450 nm with a Synergy HT Multi-Mode Microplate Reader (Biotek, Winooski, VT, USA).

Anchorage-independent cell growth was performed as previously described [32]. Briefly, MDA-MB-231 cells were plated in 0.4% agarose with CM from MLO-Y4 cells treated with ALN on top of a 0.8% agarose base supplemented with complete medium and colonies were quantified after 2 weeks.

Quantification of ATP using liquid chromatography-mass spectrometry (LC-MS)

ATP was measured from the CM containing adenosine-13C10, 15N5-triplosphate (ATP13C, 15N) as internal standard based on our previously published protocol [32] modified from Zhang et al (2011)[71]. LC-MS analysis was conducted on a Thermo Fisher Q Exactive mass spectrometer with on-line separation using a Thermo Fisher/Dionex Ultimate 3000 HPLC. Identification was based on the metabolite accurate mass (± 5 ppm) and agreement with the HPLC retention time of authentic standards. Quantification was made by integration of extracted ion chromatograms of ATP followed by comparison with the corresponding standard curves.

Fluid Flow

Fluid flow experiments were performed as described previously [36]. Briefly, the fluid flow was created by parallel-plate flow chambers separated by a gasket of defined thickness with gravity-driven fluid flow using a peristaltic pump. The circulating medium was α-MEM. The CM was collected from MLO-Y4 cells after 2 and 16 hr of shear stress level at 16 dyn/cm^2.

Conditional knockout mice and transgenic mice

Mice with floxed Cx43 gene ($Cx43^{flx/flx}$) was originally generated by Dr. Klaus Willecke's lab at the University of Bonn, Germany [72] and provided by Dr. Roberto Civitelli at Washington University. Mice with a deletion of Cx43 from osteocytes were generated using the Cre/Lox system. First, mice with floxed Cx43 gene ($Cx43^{flx/flx}$) were crossed with Cx43 heterozygous mice expressing one Cx43 allele ($Cx43^{+/-}$). We then crossed mice expressing a Cre recombinase driven by a 10-kb DMP1 promoter that leads the gene expression predominantly in osteocytes [73] (DMP1-Cre; $Cx43^{+/+}$), with $Cx43^{fl/-}$ mice to generate Cx43 osteocyte-specific conditional knockout (DMP1-Cre; $Cx43^{fl/-}$) mice. Genotyping was performed by polymerase chain reaction (PCR) techniques using genomic DNA isolated from mouse tails and corresponding primers synthesized at the UTHSCSA DNA Core Facility. Transgenic mice driven by a 10 kb-DMP1 promoter with the overexpression of Cx43 mutants, R76W and Δ130–136 were generated as previously described [38,74,75].

Intratibial injection, bioluminescence imaging and radiography

All mice were maintained in a pathogen free environment at the AAALAC-accredited UTHSCSA animal facility following the NIH Guidelines for the Care and Use of Laboratory Animals. The animal experimental protocols complied with ethical regulations and were approved by the Institutional Animal Care and Use Committee (IACUC). Four- to five-week old female C57BL/6 mice were used for the intratibial injections as previously described [32]. Animals were randomly divided into control and treated groups. The experiments were conducted blindly without revealing the information of WT and transgenic mice and identity of the mice become available after completion of the data analysis. Briefly, Py8119 cells expressing Luc-GFP (1×10^5 cells in PBS) were inoculated into the bone marrow of the right tibias. PBS was injected into the left tibias as control. For zoledronate (ZOL) treated mice, ZOL (200 μg/kg) was i.p. injected twice a week. Intratibial tumor growth was monitored with bioluminescence imaging (Xenogen IVIS-Spectrum imaging system, Alameda, CA, USA) every week starting from 3 days after tumor cell inoculation. Analysis was performed using LivingImage software (Xenogen) by measurement of photon flux (photons/sec/cm^2/steradian) with a region of interest (ROI). Tumor burden was taken by drawing an ROI around the major bioluminescence signal.

Mice were exposed with an X-ray at 35 KVP for 5 sec by using a Faxitron Digital Radiographic Inspection unit against the detector as described previously [76].

Statistical analysis

We performed preliminary experiments using 3–4 animals to compute the total number of animals required to achieve 80% power assuming two-sided testing with a significance level of 5%. Unless otherwise specified in the Figure Legends, the data are presented as the mean ± SEM of at least three determinations. Asterisks indicate the degree of significant differences compared with the controls (*, $P<0.05$; **, $P<0.01$; ***, $P<0.001$). One-way analysis of variance (ANOVA) and Student Newman-Keuls test were used to compare groups using GraphPad Prism 5.04 software (GraphPad, La Jolla, CA, USA).

Supplementary Material

Refer to Web version on PubMed Central for supplementary material.

Acknowledgments

The authors would like to thank Hongyun Cheng for technical assistance, Dr. Lesley Ellies at University of California at San Diego for providing Py8119 cells, Dr. Lynda Bonewald at University of Missouri at Kansas City for MLO-Y4 osteocytic cells, Dr. Stephen Harris at UTHSCSA for 10-kb dentin matrix protein 1 (DMP1)-Cre mice and Dr. Klaus Willecke at the University of Bonn and Dr. Roberto Civitelli for mice with floxed Cx43 gene. The work was supported by Welch Foundation grant AQ-1507 and NIH grant EY012085 to JXJ, ES022057 to LZS, and the NCI Cancer Center Grant 2 P30 CA054174-17 to Cancer Therapy and Research Center.

References

1. Welch DR, Harms JF, Mastro AM, Gay CV, Donahue HJ. Breast cancer metastasis to bone: evolving models and research challenges. J Musculoskelet Neuronal Interact. 2003; 3:30–38. [PubMed: 15758363]

2. Roodman GD. Mechanism of bone metastasis. N Engl J Med. 2004; 350:1655–1664. [PubMed: 15084698]
3. van der Pluijm G, Sijmons B, Vloedgraven H, Deckers M, Papapoulos S, Lowik C. Monitoring metastatic behavior of human tumor cells in mice with species-specific polymerase chain reaction: elevated expression of angiogenesis and bone resporption stimulators by breast cancer in bone metastases. J Bone Miner Res. 2001; 16:1077–1091. [PubMed: 11393785]
4. Theriault RL, Theriault RL. Biology of bone metastases. Cancer Control. 2012; 19:92–101. [PubMed: 22487971]
5. Place AE, Jin HS, Polyak K. The microenvironment in breast cancer progression: biology and implications for treatment. Breast Cancer Res. 2011; 13:227. [PubMed: 22078026]
6. Bonewald LF. Osteocytes as dynamic multifucntional cells. Ann N Y Acad Sci. 2007; 1116:281–290. [PubMed: 17646259]
7. Matsuo K. Cross-talk among bone cells. Curr Opin Nephrol Hypertens. 2009; 18:292–297. [PubMed: 19395964]
8. Goodenough DA, Goliger JA, Paul DL. Connexins, connexons, and intercellular communication. Annu Rev Biochem. 1996; 65:475–502. [PubMed: 8811187]
9. Goodenough DA, Paul DL. Beyond the gap: Functions of unpaired connexon channels. Nat Rev Mol Cell Biol. 2003; 4:285–294. [PubMed: 12671651]
10. Evans WH, de Vuyst E, Leybaert L. The gap junction cellular internet: connexin hemichannels enter the signaling limelight. Biochem J. 2006; 397:1–14. [PubMed: 16761954]
11. Saez JC, Berthoud VM, Branes MC, Martinez AD, Beyer EC. Plasma membrane channels formed by connexins: their regulation and functions. Physiol Rev. 2003; 83:1359–1400. [PubMed: 14506308]
12. Cherian PP, Siller-Jackson AJ, Gu S, Wang X, Bonewald LF, Sprague E, Jiang TX. Mechanical strain opens connexin 43 hemichannels in osteocytes: a novel mechanism for the release of prostaglandin. Mol Biol Cell. 2005; 16:3100–3106. [PubMed: 15843434]
13. Genetos DC, Kephart CJ, Zhang Y, Yellowley CE, Donahue HJ. Oscillating fluid flow activation of gap junction hemichannels induces ATP release from MLO-Y4 osteocytes. J Cell Physiol. 2007; 212:207–214. [PubMed: 17301958]
14. Siller-Jackson AJ, Burra S, Gu S, Xia X, Bonewald LF, Sprague E, Jiang JX. Adaptation of connexin 43-hemichannel prostaglandin release to mechanical loading. J Biol Chem. 2008; 283:26374–26382. [PubMed: 18676366]
15. Plotkin LI, Manolagas SC, Bellido T. Transduction of cell survival signals by connexin-43 hemichannels. J Biol Chem. 2002; 277:8648–8657. [PubMed: 11741942]
16. Brown SA, Guise TA. Cancer-associated bone disease. Cur Osteopor Rep. 2007; 5:120–127.
17. Mesnil M. Connexins and cancer. Biol Cell. 2002; 94:493–500. [PubMed: 12566222]
18. Mesnil M, Crespin S, Avanzo JL, Zaidan-Dagli ML. Defective gap junctional intercellular communication in the carcinogenic process. Biochim Biophys Acta. 2005; 1719:125–145. [PubMed: 16359943]
19. Cronier L, Crespin S, Strale P-O, Defamie N, Mesnil M. Gap junctions and cancer: New functions for an old story. Antioxid Redox Signal. 2009; 11:323–328. [PubMed: 18834328]
20. Laird DW, Fistouris P, Batist G, Alpert L, Huynh HT, Carystinos GD, Alaoui-Jamali MA. Deficiency of connexin43 gap junctions is an independent marker for breast tumors. Cancer Res. 1999; 59:4104–4110. [PubMed: 10463615]
21. Elzarrad MK, Haroon A, Willecke K, Dobrowolski R, Gillespie MNAl, Mehdi AB. Connexin-43 upregulation in micrometastases and tumor vasculature and its role in tumor cell attachment to pulmonary endothelium. BMC Med. 2008; 6:20. [PubMed: 18647409]
22. Stoletov K, Strnadel J, Zardouzian E, Momiyama M, Park FD, Kelber JA, Pizzo DP, Hoffman R, VandenBerg SR, Klemke RL. Role of connexins in metastatic breast cancer and melanoma brain colonization. J Cell Sci. 2013; 126:904–913. [PubMed: 23321642]
23. Avanzo JL, Mesnil M, Hernandez-Blazquez FJ, Mackowiak II, Mori CM, da Silva TC, Oloris SC, Garate AP, Massironi SM, Yamasaki H, Dagli ML. Increased susceptibility to urethane-induced lung tumors in mice with decreased expression of connexin43. Carcinogenesis. 2004; 25:1973–1982. [PubMed: 15166089]

24. Plante I, Stewart MKG, Barr K, Allan AL, Laird DW. Cx43 suppresses mammary tumor metastasis to the lung in a Cx43-mutant mouse model of human disease. Oncogene. 2011; 30:1681–1692. [PubMed: 21151177]
25. Plotkin LI, Bellido T. Bisphophonate-induced, hemichannel-mediated anti-apoptosis through the Src/ERK pathway: a gap junction-independent action of connexin43. Cell Commun Adhes. 2001; 2001:377–382. [PubMed: 12064622]
26. Riquelme MA, Kar R, Gu S, Jiang JX. Antibodies targeting extracellular domain of connexins for studies of hemichannels. Neuropharmacology. 2013; 75:525–532. [PubMed: 23499293]
27. Savariar EN, Felsen CN, Nashi N, Jiang T, Ellies LG, Steinbach P, Tsien RY, Nguyen QT. Real-time in vivo molecular detection of primary tumors and metastases with ratiometric activatable cell-penetrating peptides. Cancer Res. 2013; 73:855–864. [PubMed: 23188503]
28. Kato Y, Boskey A, Spevak L, Dallas M, Hori M, Bonewald LF. Establishment of an osteoid preosteocyte-like cell MLO-A5 that spontaneously mineralized in culture. J Bone Miner Res. 2001; 16:1622–1633. [PubMed: 11547831]
29. Cherian PP, Xia X, Jiang JX. Role of gap junction, hemichannels, and connexin 43 in mineralizing in response to intermittent and continuous application of parathyroid hormone. Cell Commun Adhes. 2008; 15:43–54. [PubMed: 18649177]
30. Kohno N. Treatment of breast cancer with bone metastasis: bisphosphonate treatment - current and future. Int J Clin Oncol. 2008; 13:18–23. [PubMed: 18307015]
31. Russell RG. Bisphosphonates: the first 40 years. Bone. 2011; 49:2–19. [PubMed: 21555003]
32. Zhou JZ, Riquelme MA, Gao X, Ellies LG, Sun LZ, Jiang JX. Differential impact of adenosine nucleotides released by osteocytes on breast cancer growth and bone metastasis. Oncogene. 2015; 34:1831–1842. [PubMed: 24837364]
33. Aarden EM, Burger EH, Nijweide PJ. Function of osteocytes in bone. J Cell Biochem. 1994; 55:287–299. [PubMed: 7962159]
34. Klein-nulend J, Bakker AD, Bacabac RG, Vatsa A, Weinbaum S. Mechanosensation and transduction in osteocytes. Bone. 2013; 54:182–190. [PubMed: 23085083]
35. Jiang JX, Siller-Jackson AJ, Burra S. Roles of gap junctions and hemichannels in bone cell functions and in signal transmission of mechanical stress. Front Biosci. 2007; 12:1450–1462. [PubMed: 17127393]
36. Cheng B, Zhao S, Luo J, Sprague E, Bonewald LF, Jiang JX. Expression of functional gap junctions and regulation by fluid flow shear stress in osteocyte-like MLO-Y4 cells. J Bone Miner Res. 2001; 16:249–259. [PubMed: 11204425]
37. Bivi N, Condon KW, Allen MR, Farlow N, Passeri G, Brun LR, Rhee Y, Bellido T, Plotkin LI. Cell autonomous requirement of connexin 43 for osteocyte survival: consequences for endocortical resorption and periosteal bone formation. J Bone Miner Res. 2012; 27:374–389. [PubMed: 22028311]
38. Xu H, Gu S, Riquelme MA, Burra S, Callaway D, Cheng H, Guda T, Schmitz J, Fajardo RJ, Werner SL, Zhao H, Shang P, Johnson ML, Bonewald LF, Jiang JX. Connexin 43 channels are essential for normal bone structure and osteocyte viability. J Bone Miner Res. 2015; 30:436–448. [PubMed: 25270829]
39. Joyce JA, Pollard JW. Microenvironmental regulation of metastasis. Nat Rev Cancer. 2009; 9:239–252. [PubMed: 19279573]
40. Liotta LA, Kohn EC. The microenvironment of the tumour-host interface. Nature. 2001; 411:375–379. [PubMed: 11357145]
41. Paget S. The distribution of secondary growths in cancer of the breast. Lancet. 1889; 1:571–573.
42. Bonewald LF. The amazing osteocyte. J Bone Miner Res. 2011; 26:229–238. [PubMed: 21254230]
43. Bennett MV, Garre JM, Orellana JA, Bukauskas FF, Nedergaard M, Saez JC. Connexin and pannexin hemichannels in inflammatory responses of glia and neurons. Brain Res. 2012; 1487:3–15. [PubMed: 22975435]
44. Calder BW, Matthew RJ, Bainbridge H, Fann SA, Gourdie RG, Yost MJ. Inhibition of connexin 43 hemichannel-mediated ATP release attenuates early inflammation during the foreign body response. Tissue Eng Part A. 2015; 21:1752–1762. [PubMed: 25760687]

45. Stains JP, Civitelli R. Gap junctions in skeletal development and function. Biiochim Biophys Acta. 2005; 1719:69–81.
46. Laird DW. Life cycle of connexins in health and disease. Biochem J. 2006; 394:527–543. [PubMed: 16492141]
47. Chung DJ, Castro CH, Watkins M, Stains JP, Chung MY, Szejnfeld VL, Willecke K, Theis M, Civitelli R. Low peak bone mass and attenuated response to parathyroid hormone in mice with an osteoblast-specific deletion of connexin43. J Cell Sci. 2006; 119:4187–4198. [PubMed: 16984976]
48. Bivi N, Pacheco-Costa R, Brun LR, Murphy TR, Farlow NR, Robling AG, Bellido T, Plotkin LI. Absence of Cx43 selectively from osteocytes enhances responsiveness to mechanical force in mice. J Orthop Res. 2013; 31:1075–1081. [PubMed: 23483620]
49. Zhang Y, Paul EM, Sathyendra V, Davison A, Sharkey N, Bronson S, Srinivasan S, Gross TS, Donahue HJ. Enhanced osteoclastic resorption and responsiveness to mechanical load in gap junction deficient bone. PLos One. 2011; 6:e23516. [PubMed: 21897843]
50. Loiselle AE, Paul EM, Lewis GS, Donahue HJ. Osteoblast and osteocyte-specific loss of Connexin43 results in delayed bone formation and healing during murine fracture healing. J Orthop Res. 2013; 31:147–154. [PubMed: 22718243]
51. Orellana JA, Shoji KF, Abudara V, Ezan P, Amigou E, Sáez PJ, Jiang JX, Naus CC, Sáez JC, Giaume C. Amyloid β-induced death in neurons involves glial and neuronal hemichannels. J Neurosci. 2011; 31:4962–4977. [PubMed: 21451035]
52. Orellana JA, Froger N, Ezan P, Jiang JX, Bennett MV, Naus CC, Giaume CSáez JC. ATP and glutamate released via astroglial connexin 43hemichannels mediate neuronal death through activation of pannexin 1 hemichannels. J Neurochem. 2011; 118:826–840. [PubMed: 21294731]
53. Orellana JA, Sáez PJ, Cortés-Campos C, Elizondo RJ, Shoji KF, Contreras-Duarte S, Figueroa V, Velarde V, Jiang JX, Nualart F, Sáez JC, Garcia MA. Glucose increase intracellular free Ca(2+) in tanycytes via ATP released through connexin 43 hemichannels. Glia. 2012; 60:53–68. [PubMed: 21987367]
54. Kato Y, Windle JJ, Koop BA, Mundy GR, Bonewald LF. Establishment of an osteocyte-like cell line, MLO-Y4. J Bone Miner Res. 1997; 12:2014–2023. [PubMed: 9421234]
55. Shabbir M, Burnstock G. Purinergic receptor-mediated effects of adenosine 5'-triphosphate in urological malignant diseases. Int J Urol. 2009; 16:143–150. [PubMed: 19183233]
56. White N, Burnstock G. P2 receptors and cancer. Trends Pharmacol Sci. 2006; 27:211–217. [PubMed: 16530853]
57. Rapaport E, Fishman RF, Gercel C. Growth inhibition of human tumor cells in soft-agar cultures by treatment with low levels of adenosine 5'-triphosphate. Cancer Res. 1983; 43:4402–4406. [PubMed: 6871873]
58. Saez JC, Contreras JE, Bukauskas FF, Retamal MA, Bennett MVL. Gap junction hemichannels in astrocytes of the CNS. Acta Physiol Scand. 2003; 179:9–22. [PubMed: 12940934]
59. Plotkin LI. Connexin 43 hemichannels and intracellular signaling in bone cells. Front Physiol. 2014; 5:131. [PubMed: 24772090]
60. D'hondt C, Iyyathurai J, Himpens B, Leybaert L, Bultynck G. Cx43-hemichannel function and regulation in physiology and pathophysiology: insights from the bovine corneal endothelial cell system and beyond. Front Physiol. 2014; 5:348. [PubMed: 25309448]
61. Sterling JA, Guelcher SA. Bone structural components regulating sites of tumor metastasis. Curr Osteoporos Rep. 2011; 9:89–95. [PubMed: 21424744]
62. Milne HM, Wallman KE, Gordon S, Courneya KS. Effects of a combined aerobic and resistance exercise program in breast cancer survivors: a randomized controlled trial. Breast Cancer Res Treat. 2008; 108:279–288. [PubMed: 17530428]
63. Schwartz AL, Winters-Stone K, Gallucci B. Exercise effects on bone mineral density in women with breast cancer receiving adjuvant chemotherapy. Oncol Nurs Forum. 2007; 34:627–633. [PubMed: 17573321]
64. Holick CN, Newcomb PA, Trentham-Dietz A, Titus-Ernstoff L, Bersch AJ, Stampfer MJ, Baron JA, Egan KM, Willett WC. Physical activity and survival after diagnosis of invasive breast cancer. Cancer Epidemiol Biomarkers Prev. 2008; 17:379–386. [PubMed: 18250341]

65. Irwin ML, McTiernan A, Manson JE, Thomson CA, Sternfeld B, Stefanick ML, Wactawski-Wende J, Craft L, Lane D, Martin LW, Chlebowski R. Physical activity and survival in postmenopausal women with breast cancer: results from the women's health initiative. Cancer Prev Res (Phila). 2011; 4:522–529. [PubMed: 21464032]

66. Lynch ME, Brooks D, Mohanan S, Lee MJ, Polamraju P, Dent K, Bonassar LJ, van der Meulen MC, Fischbach C. In vivo tibial compression decreases osteolysis and tumor formation in a human metastatic breast cancer model. J Bone Miner Res. 2013; 28:2357–2367. [PubMed: 23649605]

67. Kretschmann KL, Welm AL. Mouse models of breast cancer metastasis to bone. Cancer Metastasis Rev. 2012; 31:579–583. [PubMed: 22706780]

68. Xu H, Gu S, Riquelme MA, Burra S, Callaway D, Cheng H, Guda T, Schmitz J, Fajardo RJ, Werner SL, Zhao H, Shang P, Johnson ML, Bonewald LF, Jiang JX. Connexin 43 Channels are Essential for Normal Bone Structure and Osteocyte Viability. J Bone Miner Res. 2014

69. Dbouk HA, Mroue RM, El Sabban ME, Talhouk RS. Connexins: a myriad of functions extending beyond assembly of gap junction channels. Cell Commun Signal. 2009; 7:4. [PubMed: 19284610]

70. Zhou JZ, Jiang JX. Gap junction and hemichannel-independent actions of connexins on cell and tissue functions--an update. FEBS Lett. 2014; 588:1186–1192. [PubMed: 24434539]

71. Zhang W, Tan S, Paintsil E, Dutschman GE, Gullen EA, Chu E, Cheng YC. Analysis of deoxyribonucleotide pools in human cancer cell lines using a liquid chromatography coupled with tandem mass spectrometry technique. Biochem Pharmacol. 2011; 82:411–417. [PubMed: 21620803]

72. Theis M, de Wit C, Schlaeger TM, Eckardt D, Krüger O, Döring B, Risau W, Deutsch U, Pohl U, Willecke K. Endothelium-specific replacement of the connexin43 coding region by a lacZ reporter gene. Genesis. 2001; 29:1–13. [PubMed: 11135457]

73. Yang W, Kalajzic I, Lu Y, Guo D, Harris MA, Gluhak-Heinrich J, Kotha S, Bonewald LF, Feng JQ, Rose DW, Harris SE. Identification of an osteocyte-specific mechanically regulated region of the dentin matrix protein 1 gene. J Biol Chem. 2005; 280:20680–20690. [PubMed: 15728181]

74. Xu H, Gu S, Riquelme MA, Burra S, Callaway D, Cheng H, Guda T, Schmitz J, Fajardo RJ, Werner SL, Zhao H, Shang P, Johnson ML, Bonewald LF, Jiang JX. Connexin 43 Channels are Essential for Normal Bone Structure and Osteocyte Viability. J Bone Miner Res. 2014

75. Xu H, Gu S, Riquelme MA, Burra S, Callaway D, Cheng H, Guda T, Schmitz J, Fajardo RJ, Werner SL, Zhao H, Shang P, Johnson ML, Bonewald LF, Jiang JX. Connexin 43 Channels are Essential for Normal Bone Structure and Osteocyte Viability. J Bone Miner Res. 2014

76. Guise TA, Yin JJ, Taylor SD, Kumagai Y, Dallas M, Boyce BF, Yoneda T, Mundy GR. Evidence for a causal role of parathyroid hormone-related protein in the pathogenesis of human breast cancer-mediated osteolysis. J Clin Invest. 1996; 98:1544–1549. [PubMed: 8833902]

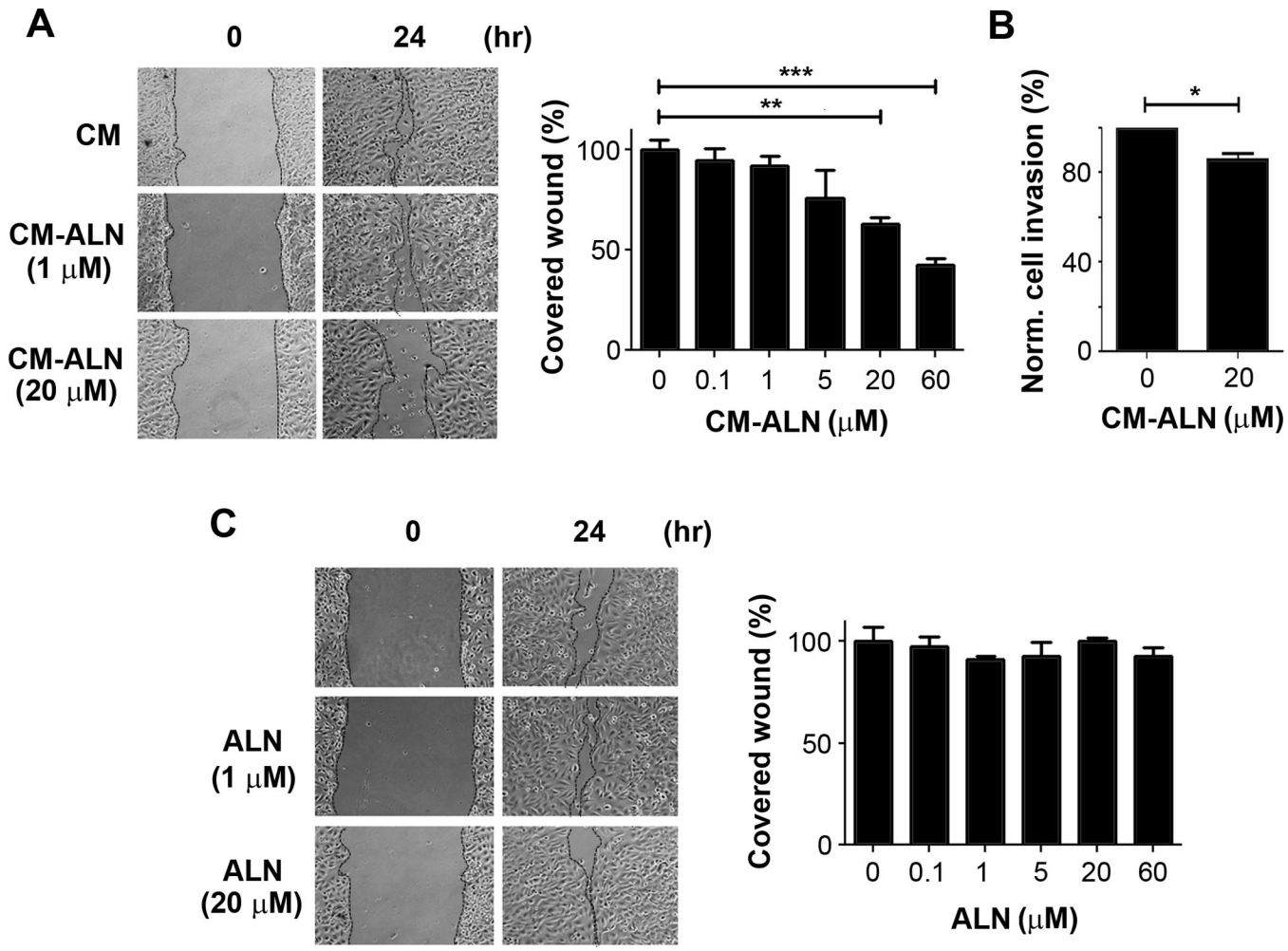

Figure 1.

The CM from ALN-treated osteocytes inhibits human breast cancer cell migration and invasion. MDA-MB-231 breast cancer cells were cultured to confluence and a wound was created. The gap areas between scratches were quantified by using ImageJ software. **(A)** MDA-MB-231 cells were incubated with the CM collected from MLO-Y4 cells (CM-ALN) and treated with ALN at various concentrations. Percentage of total covered wound was quantified (right panel). **(B)** MDA-MB-231 cells were incubated with CM collected from MLO-Y4 cells treated with 20 μM ALN (CM-ALN). Percentage of total invading cells was quantified. **(C)** MDA-MB-231 cells were incubated with the CM collected from MLO-Y4 cells without ALN, but ALN was added at various concentrations (0–60 μM) directly to MDA-MB-231 cells. Percentage of total covered wound was quantified (right panel). All data were presented as mean±SEM, n=3. *, $P<0.05$; **, $P<0.01$; ***, $P<0.001$.

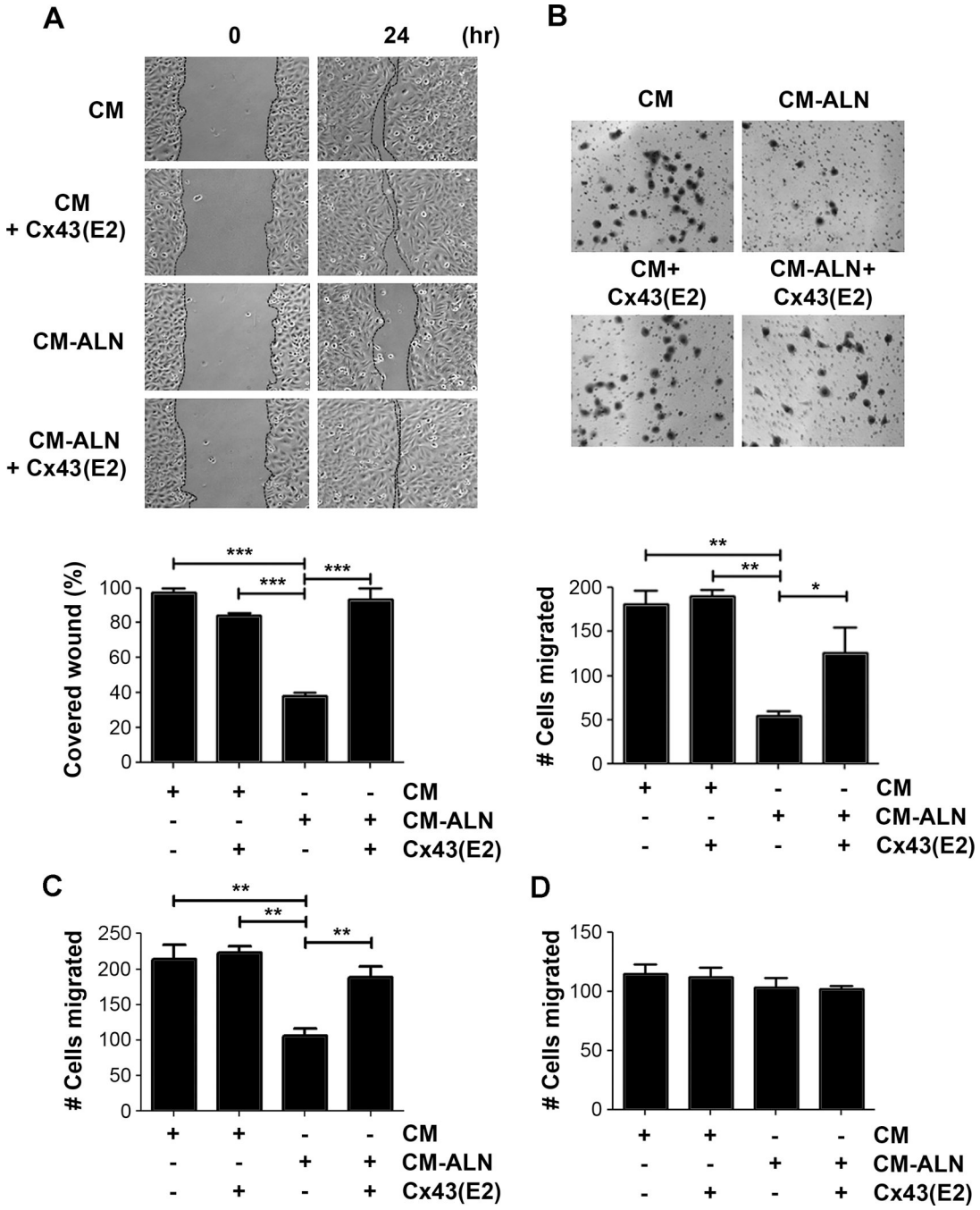

Figure 2.

Blocking osteocytic Cx43 hemichannels attenuates the inhibitory effect of CM from ALN-treated osteocytes on the migration of breast cancer cells. MDA-MB-231 cells were incubated with CM collected from MLO-Y4 cells treated with (CM-ALN) or without (CM) 20 μM ALN and 1 μg/ml Cx43(E2) antibody **(A and B). (A)** Wound healing migration assay was performed and percentage of total covered wound was quantified (lower panel). **(B)** The transwell migration assay was performed and the cells migrated across the transwell filter were quantified (lower panel). **(C)** Py8119 cells were incubated with CM collected from

MLO-Y4 cells treated with (CM-ALN) or without (CM) 20 μM ALN and 1 μg/ml Cx43(E2) antibody. The cells migrated through the transwell filter were quantified. **(D)** MDA-MB-231 cells were incubated in CM collected from osteoblastic MLO-A5 cells treated with (CM-ALN) or without (CM) 20 μM ALN and 1 μg/ml Cx43(E2) antibody. The cells migrated in the transwell migration assay were quantified. All data were presented as mean±SEM, n=3. *, $P<0.05$; **, $P<0.01$; ***, $P<0.001$.

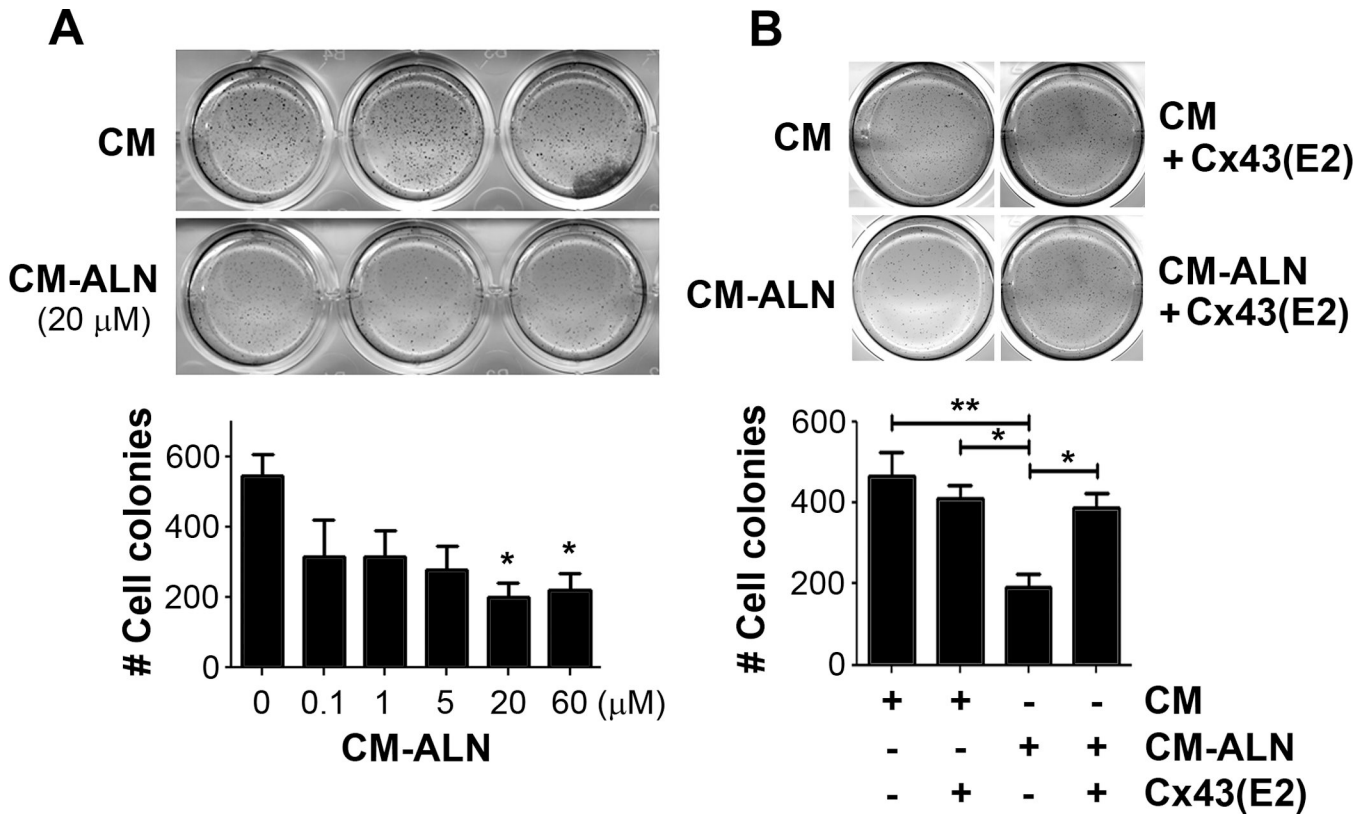

Figure 3.

The anchorage-independent growth of breast cancer cells is inhibited by CM from ALN-treated osteocytes and attenuated with Cx43(E2) antibody. **(A)** MDA-MB-231 cells plated on soft agar were incubated with CM collected from MLO-Y4 cells treated with ALN (CM-ALN) at various concentrations. Cells growing on soft agar plates were quantified (bottom panel). **(B)** MDA-MB-231 cells plated on soft agar were incubated with CM collected from MLO-Y4 cells treated with (CM-ALN) or without (CM) 20 μM ALN and 1 μg/ml Cx43(E2) antibody for 48 hr. Cells growing on soft agar plates were quantified (bottom panel). All data were presented as mean±SEM, n=3. *, $P<0.05$; **, $P<0.01$.

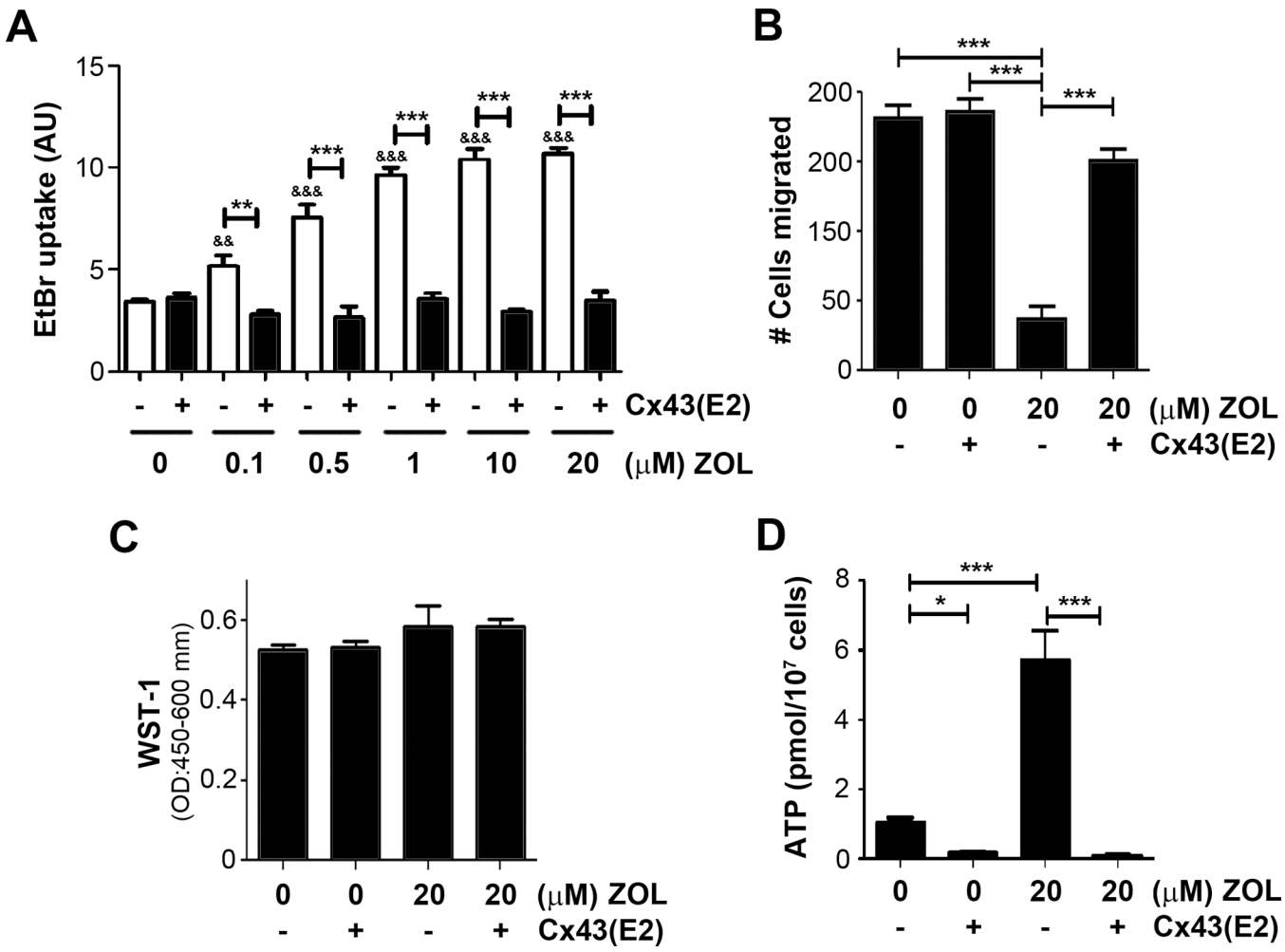

Figure 4.

Osteocytic Cx43 hemichannel opening with ATP release induced by ZOL is blocked by Cx43(E2) antibody. **(A)** MLO-Y4 cells were treated with various concentrations of ZOL with or without 1 μg/ml Cx43(E2) antibody. EtBr dye uptake was conducted and quantified, As compared to non-treated basal level of uptake, $^{\&\&}$, $P<0.01$ and $^{\&\&\&}$, $P<0.001$. **(B)** MDA-MB-231 cells were incubated with CM collected from MLO-Y4 cells treated with (CM-ALN) or without (CM) 20 μM ZOL and 1 μg/ml Cx43(E2) antibody. The cells migrated through the transwell filter were quantified. **(C)** The cell proliferation was analyzed by WST-1 assay. **(D)** CM was collected from MLO-Y4 cells treated with (CM-ALN) or without (CM) 20 μM ZOL and 1 μg/ml Cx43(E2) antibody for 24 hr and ATP was measured using LC-MS. All data were presented as mean±SEM, n=3. *, $P<0.05$; **, $P<0.01$; ***, $P<0.001$.

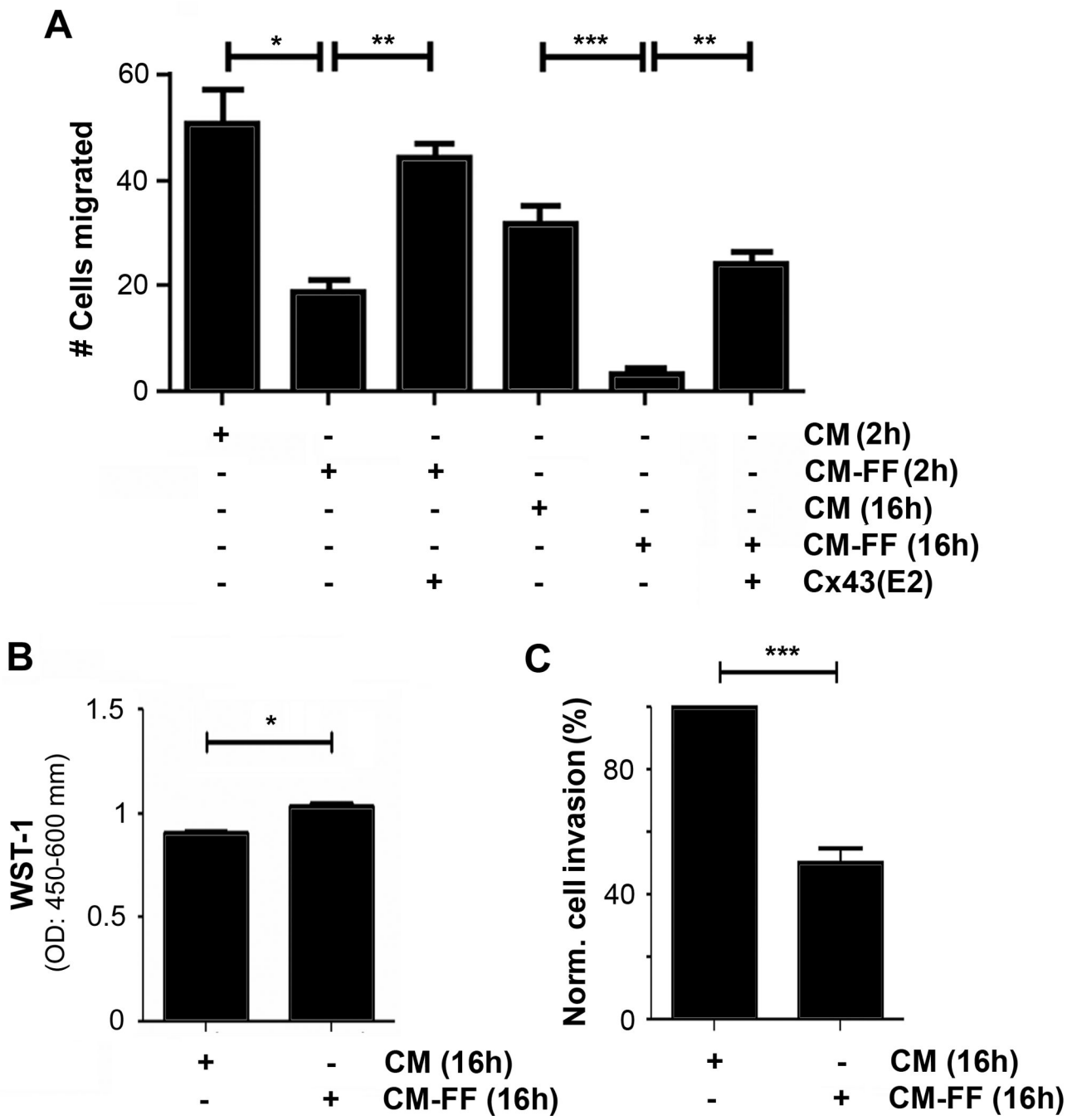

Figure 5.

The opening of Cx43 hemichannels in osteocytes by FFSS inhibits the migration of breast cancer cells. **(A)** MDA-MB-231 cells were incubated with media collected from MLO-Y4 cells treated with (CM-FF) or without (CM) 16 dyn/cm^2 FFSS for 2 hr or 16 hr and 1 μg/ml Cx43(E2) antibody. The cells migrated through the transwell filter were quantified. **(B)** The cell proliferation was analyzed by WST-1 assay. **(C)** MDA-MB-231 cells were incubated with media collected from MLO-Y4 cells treated (CM-FF) with or without (CM) 16

dyn/cm^2 FFSS for 16 hr. Percentage of total invading cells was quantified. All data were presented as mean±SEM, n=3. *, $P<0.05$; **, $P<0.01$; ***, $P<0.001$.

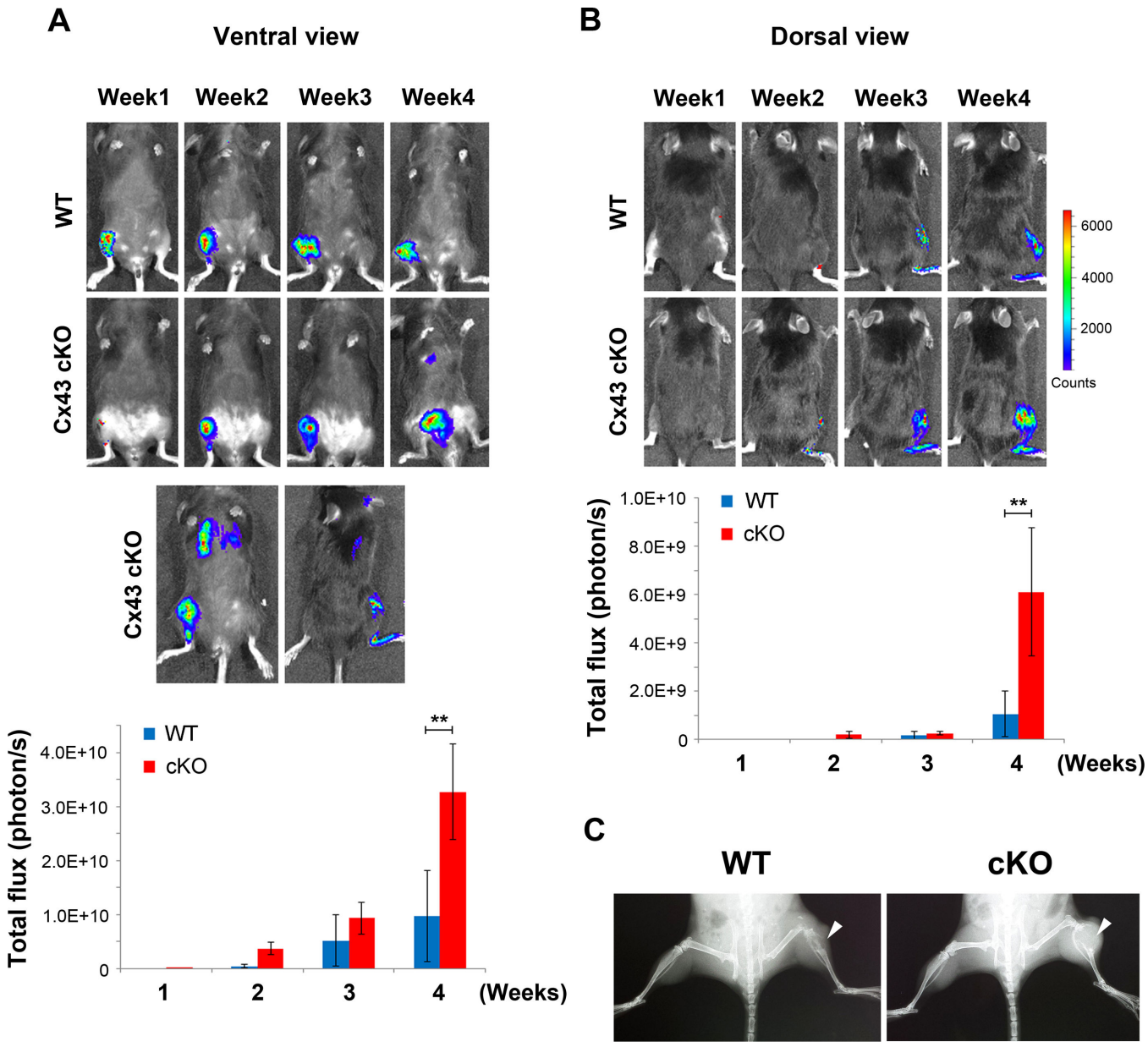

Figure 6.

Osteocyte-specific Cx43 cKO mice exhibit increased growth of mouse mammary carcinoma cells in bone. Py8119/Luc-GFP cells were injected into the right tibias of Cx43 cKO and WT female mice. Total photon flux was taken once a week after tumor cell injection. Ventral **(A)** and **(B)** dorsal view (top panels) of whole body imaging is shown. Representative images of mice with tumor spread to the lungs and brain shown (**A**, middle panel). Luciferase signals were quantified by Living Image 3.2 (bottom panels). **(C)** Representative X-ray radiographs of right tibia injected with Py8119 cells. The arrows indicate where the tumor cells were injected. Data were presented as mean±SEM, n=7 per group. **, $P<0.01$.

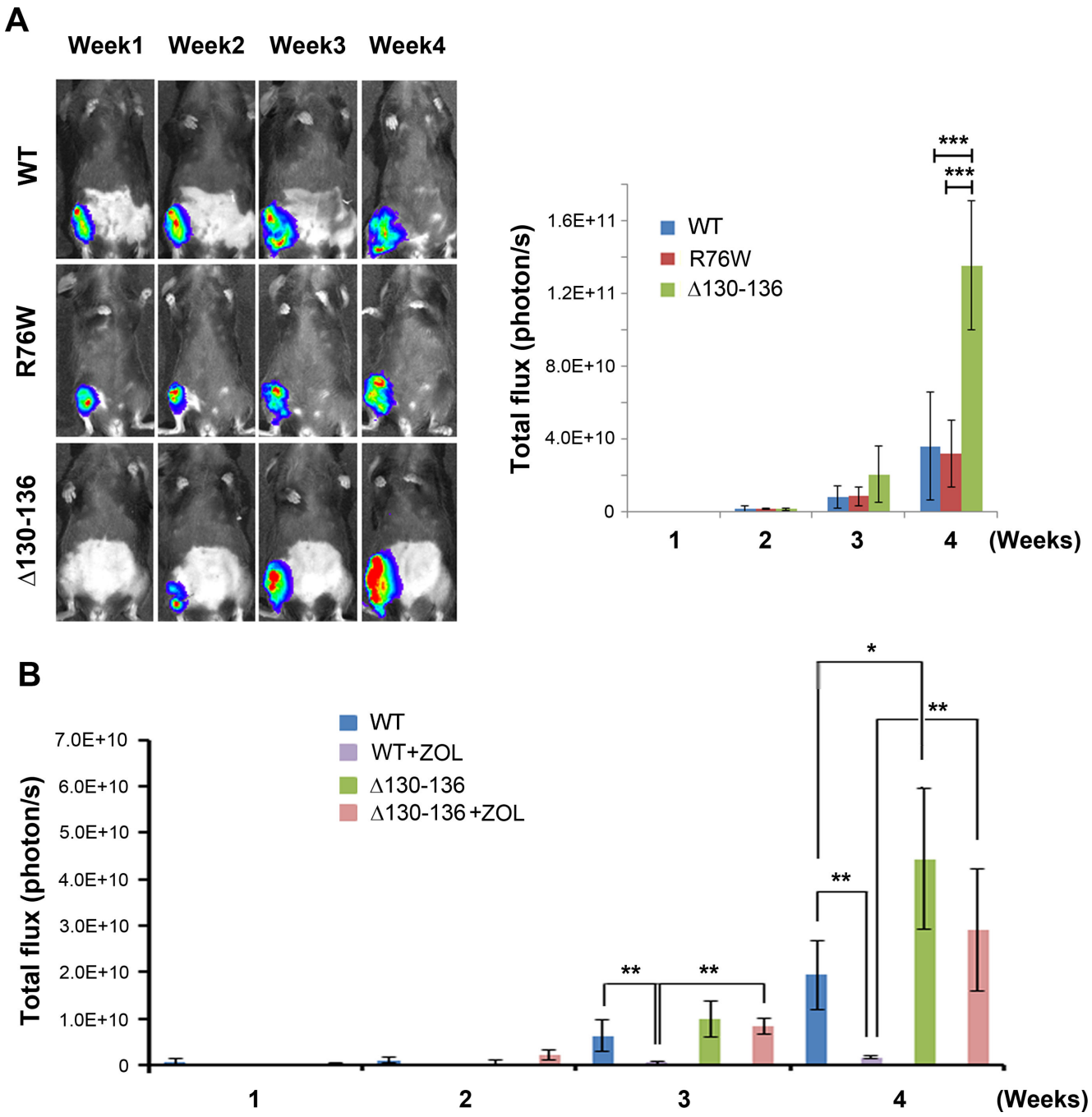

Figure 7.

Transgenic mice expressing Cx43(Δ130–136) in osteocytes displayed increased growth of Py8119 cells and attenuated the inhibitory effect of ZOL on tumor growth. **(A)** Py8119/Luc-GFP cells were injected into the right tibias of R76W, Δ130–136 and WT female mice. Total photon flux was taken once a week after tumor cell injection. Ventral view (left panel) of whole body imaging is shown. Luciferase signals were quantified by Living Image 3.2 (right panels). **(B)** Py8119/Luc-GFP cells were injected into the right tibias of WT (left panel) and Δ130–136 (right panel) female mice and saline or ZOL (200 μg/kg) was i.p. injected twice a

week beginning on the day of tumor cell inoculation. Data were presented as mean±SEM, n=7–8 per group. *, $P<0.05$; **, $P<0.01$; ***, $P<0.001$.